

# Synthesis and Characterization of Fe<sub>3</sub>O<sub>4</sub> Coated on APTES as Carriers for Morin-Anticancer Drug

Bassam Saif<sup>1</sup>, Congli Wang<sup>1</sup>, Dong Chuan<sup>2</sup>, Shaomin Shuang<sup>1</sup>

<sup>1</sup>School of Chemistry and Chemical Engineering, Shanxi University, Taiyuan, China

<sup>2</sup>Research Center of Environmental Science and Engineering, Shanxi University, Taiyuan, China

Email: [smshuang@sxu.edu.cn](mailto:smshuang@sxu.edu.cn)

Received 30 August 2015; accepted 18 October 2015; published 21 October 2015

Copyright © 2015 by authors and Scientific Research Publishing Inc.

This work is licensed under the Creative Commons Attribution International License (CC BY).

<http://creativecommons.org/licenses/by/4.0/>



Open Access

---

## Abstract

Morin (MR) is an anticancer drug present in fruits and Chinese herbs. Fe<sub>3</sub>O<sub>4</sub> magnetic nanoparticles (MNPs) coated on 3-aminopropyl triethoxysilane (APTES) were synthesized (MNPs-APTES) as carriers for MR. The characterization of drug delivery system was confirmed by Fourier Transform Infrared (FTIR), Transmission Electron Microscope (TEM), X-Ray Diffraction (XRD), dynamic light scattering (DLS), and vibrating sample magnetometer (VSM). The adsorbed APTES on the magnetite surface (MNPs-APTES) was examined by FTIR. The TEM image showed that the average particle size is obtained to be about 26.7 nm for MNPs-APTES. The MR loading and release behavior of MNPs-APTES were studied and the results showed that up to 60% of the adsorbed drug was released within 4 h. In summary, the MNPs-APTES nanocarriers are based on the results, promising for targeted morin drug delivery.

## Keywords

Magnetic Nanoparticles, Drug Delivery, Flavonoid, Morin

---

## 1. Introduction

With dramatic progress in biomaterials and biomedical applications, huge amount of new and more promising drugs are discovered and designed. Scientists and researchers are now trying to develop mechanisms that allow drugs to go directly to a targeted area of the human body. The success of chemotherapy depends on the drug, its dosage, as well as how it is delivered to its target [1]. Nowadays, nanoparticles (NPs) such as Fe<sub>3</sub>O<sub>4</sub> magnetic nanoparticles (MNPs) have gained significant attention due to their potential biomedical applications such as

immunoassay [2], magnetic resonance imaging [3], bioseparators [4] and targeted drug delivery via applying an external magnetic field [5]. At the same time, MNPs also have attractive properties, such as biocompatibility [6] and low toxicity [7]. In addition, magnetic nanoparticles are easily obtained via various techniques such as micro-emulsion, ultra sound irradiation technology, and co-precipitation [8] [9].  $\text{Fe}_3\text{O}_4$  core serves as a carrier for magnetic targeting, while silica coating such as 3-aminopropyltriethoxysilane (APTES) on the  $\text{Fe}_3\text{O}_4$  NPs offers sites for further modifications [10]. This APTES can bind to MNPs by adsorption or covalent bonding (MNPs-APTES), and through the active amino group in its structure it is able to combine with anti-cancer drug morin (MR). Morin (3,5,7,2',4'-pentahydroxyflavone, **Figure 1**), is a member of the flavonoids groups that has been reported as an important agent effective chemotherapeutic used for the treatment of cancer [11]. Furthermore, numerous reports suggest that morin has a wide range of therapeutic applications such as anti-inflammation [12], antioxidant [13], it induces apoptosis in hepatocellular carcinogenesis model [14], and xanthine oxidase inhibition activity [15]. In this study,  $\text{Fe}_3\text{O}_4$  magnetic nanoparticles were fabricated by co-precipitation method and coated with APTES. Then, this MNPs-APTES were used as drug carriers. FTIR, TEM, XRD, DLS and VSM were used to characterize the synthesized nanoparticles. MR drug is loaded onto it and its loading and *in vitro* drug release profile was studied.

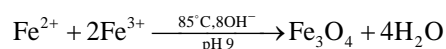
## 2. Experimental

### 2.1. Chemicals

3-aminopropyltriethoxysilane (APTES) was obtained from Aladdin Company Inc. Ferric chloride hexa-hydrate ( $\text{FeCl}_3 \cdot 6\text{H}_2\text{O}$ ) and ferrous chloride tetrahydrate ( $\text{FeCl}_2 \cdot 4\text{H}_2\text{O}$ ) were purchased from Tianjin Guangfu Fine Chemical Industry Research Institute. Dimethylsulfoxide (DMSO) was purchased from Shanghai Chemical Reagent Co. Ltd. and morin was purchased from Tianjin Fuyu Fine Chemical Co. Ltd. Deionized water was used in all of the experiments.

### 2.2. Preparation of $\text{Fe}_3\text{O}_4$ Nanoparticles (MNPs)

The co-precipitation method was used for the synthesis of  $\text{Fe}_3\text{O}_4$  nanoparticles [16]. In the typical experimental procedure, 8.11 g of iron (III) chloride hexahydrate ( $\text{FeCl}_3 \cdot 6\text{H}_2\text{O}$ ), 5.96 g of iron (II) chloride tetrahydrate ( $\text{FeCl}_2 \cdot 4\text{H}_2\text{O}$ ) were added into three-necked flask contains 200 mL deionized water previously heated to  $85^\circ\text{C}$ . The system was purged with  $\text{N}_2$  and the mixture of the iron solution was stirred followed by the slow addition of ammonia ( $\text{NH}_3 \cdot \text{H}_2\text{O}$ ) to bring the pH 9. During the reaction process, the temperature was maintained at  $85^\circ\text{C}$  and (pH 9). The precipitate was washed several times with deionized water and ethanol. The as-prepared  $\text{Fe}_3\text{O}_4$  powder was obtained after 24 h drying in vacuum condition at  $40^\circ\text{C}$ . This can be explained as:



### 2.3. Preparation of APTES Coated MNPs (MNPs-APTES)

APTES coated MNPs were synthesized using Cao *et al.* method [17]. Briefly, 0.3 g of  $\text{Fe}_3\text{O}_4$  was dispersed into a mixture of 4 mL deionized water and 600 mL absolute ethanol by ultrasonic vibration for 30 min. Then, 1.2

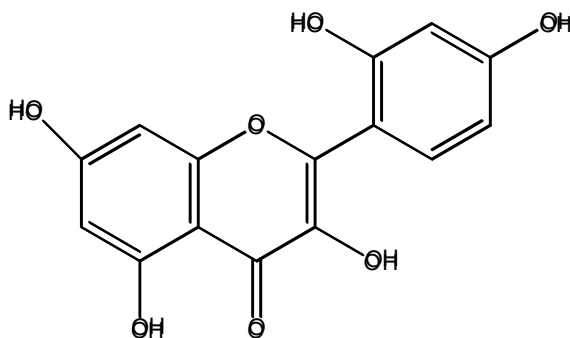


**Figure 1.** Chemical structure of morin.

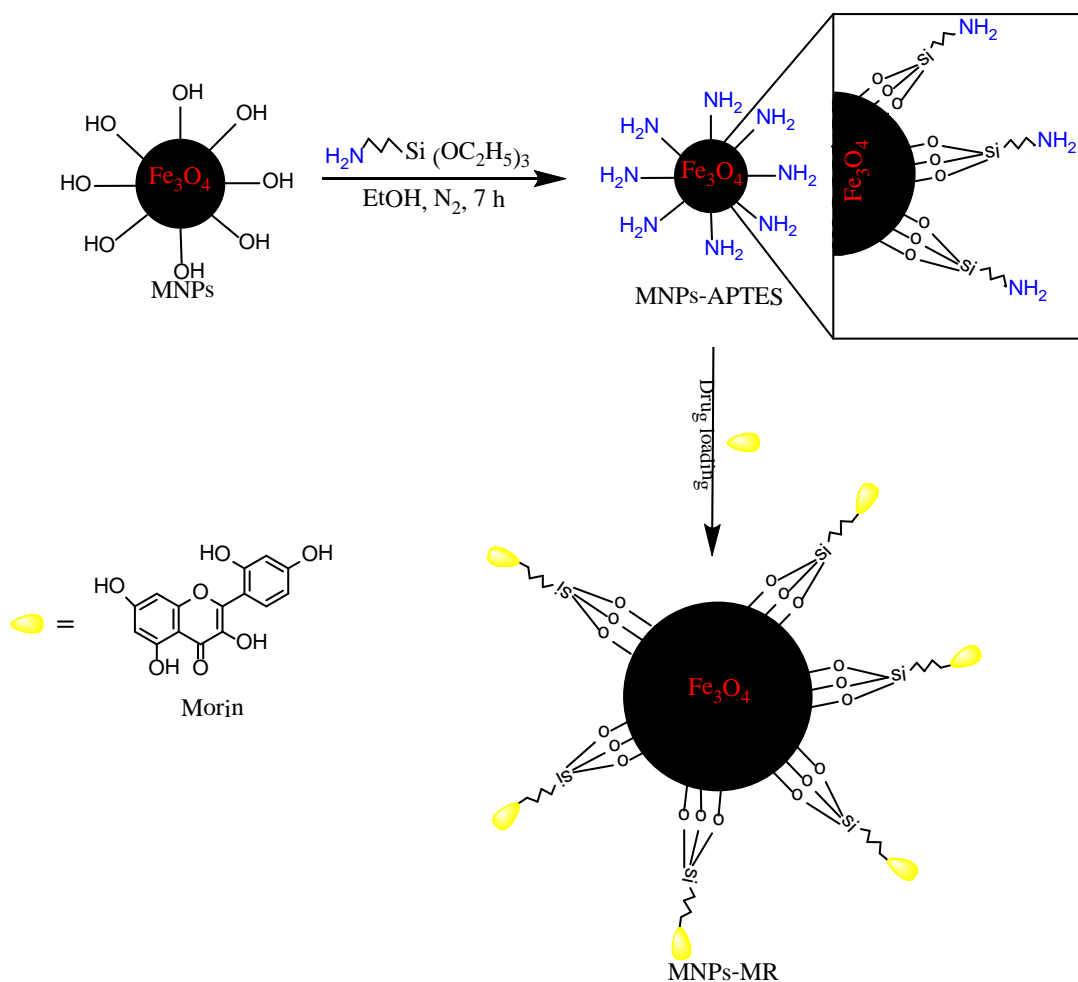
mL of APTES was added into the mixture under constant mechanical stirring for 7 h. The resulting functionalized MNPs-APTES nanoparticles were isolated by a magnet, then washed with ethanol and dried at 40°C under vacuum for 24 h. The schematic representation of the preparation procedure of MNPs-APTES is illustrated in Scheme 1.

#### 2.4. Morin (MR) Drug Loading and Release Studies

The drug loading was measured using UV-Vis spectrophotometry. The anti-cancer drug (MR) loading was carried out by dispersing 50 mg of magnetic nanoparticles coated APTES in (5 mL DMSO with 20 mL ethanol) solution containing MR (12 - 81 mg/mL). The solutions stirring at room temperature for 24 h allow partitioning of the drug into the MNPs-APTES. Then, the particles were magnetically separated from the solution by an external magnet, and MR content in the solution was determined at 388 nm. The drug loading was determined as the difference between the initial MR concentration and the MR concentration in the supernatant. The drug loaded magnetic nanoparticles were then magnetically separated and dried. The MR release study was obtained by investigated the dried drug loaded nanoparticles (10 mg) in 250 mL PBS (pH 5.2 and 7.4) at 37°C for 4 h under stirring. At given time intervals, 4 mL samples were withdrawn from the incubation medium and the amount of drug release was estimated at 388 nm by UV-Vis spectrophotometry.

#### 2.5. Characterization

The Fourier transformed infrared spectroscopy (FTIR, 8400 S Shimadzu) spectra were obtained using the KBr



Scheme 1

pellet method. The particle size and morphology of the magnetic nanoparticles (MNPs and MNPs-APTES) were determined by transmission electron microscopy (TEM, JEM-1011). Magnetic nanoparticles were also analyzed by X-Ray diffraction (XRD, Rigaku D max-2400). The hydrodynamic diameter measured by dynamic light scattering (DLS, Nano-ZS 90) for MNPs-APTES. Finally, the magnetic properties were investigated with vibrating sample magnetometer (VSM, Lakeshore).

### 3. Results and Discussion

#### 3.1. FTIR Studies

FT-IR spectra of MNP, APTES-MNP and morin binded on APTES-MNP are shown in **Figure 2**. The strong absorption at  $584\text{ cm}^{-1}$  in curves a, b and c are attributed to the stretch of Fe-O [18], the peak at  $3425\text{ cm}^{-1}$  is attributed to the stretching vibrations of OH adsorbed on the surface of the  $\text{Fe}_3\text{O}_4$  nanoparticle (**Figure 2(a)**). APTES is absorbed on the magnetite nanoparticles surfaces by Fe-O-Si bands, the coating of APTES is established by the presence of stretching vibration of  $\text{CH}_2$  bonds on aminopropyl group appeared at 2922 and  $2850\text{ cm}^{-1}$  which confirmed the binding of APTES molecules at the surface of magnetite (APTES-MNP) [19], and the bands around 1089 and  $1193\text{ cm}^{-1}$  corresponded to the presence of SiO-H and Si-O-Si groups in **Figure 2(b)**. [17]. Additionally, the peaks at 1623 and  $3403\text{ cm}^{-1}$  showed the presence of the N-H stretching vibrations and bending mode of free- $\text{NH}_2$  group, respectively. In **Figure 2(c)**, the appearance of new bands at 1353, 1451, 1506, 1606, 1653, 3475 and  $3296\text{ cm}^{-1}$  in the FTIR graph indicates the presence of morin. A band appeared at  $1228\text{ cm}^{-1}$  due to the formation of C-N bond between  $\text{NH}_2$  group in APTES and OH group present on the morin with the elimination of water.

#### 3.2. TEM Studies

The morphology of the MNPs and MNPs-APTES were characterized using a transmission electron microscope (TEM) images shown in **Figure 3**. **Figure 3(a)** showed that the MNPs possess spherical morphology with an average diameter of about 14.2 nm in size. After surface coating with APTES, the TEM micrograph on **Figure 3(b)** clearly observed the successful synthesis of MNPs-APTES and, the particle size was around 26.7 nm. In addition, the particle size of MNPs-APTES was obtained as 44 nm using dynamic light scattering (DLS)

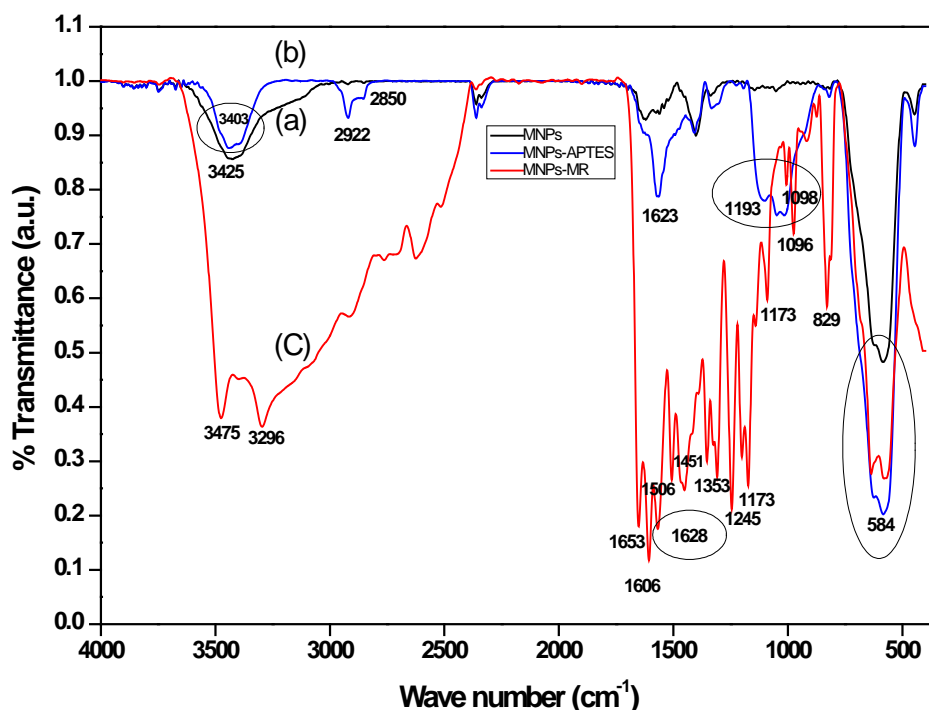


**Figure 2.** FTIR spectra of (a) MNPs, (b) MNPs-APTES, and (c) MNPs-MR.

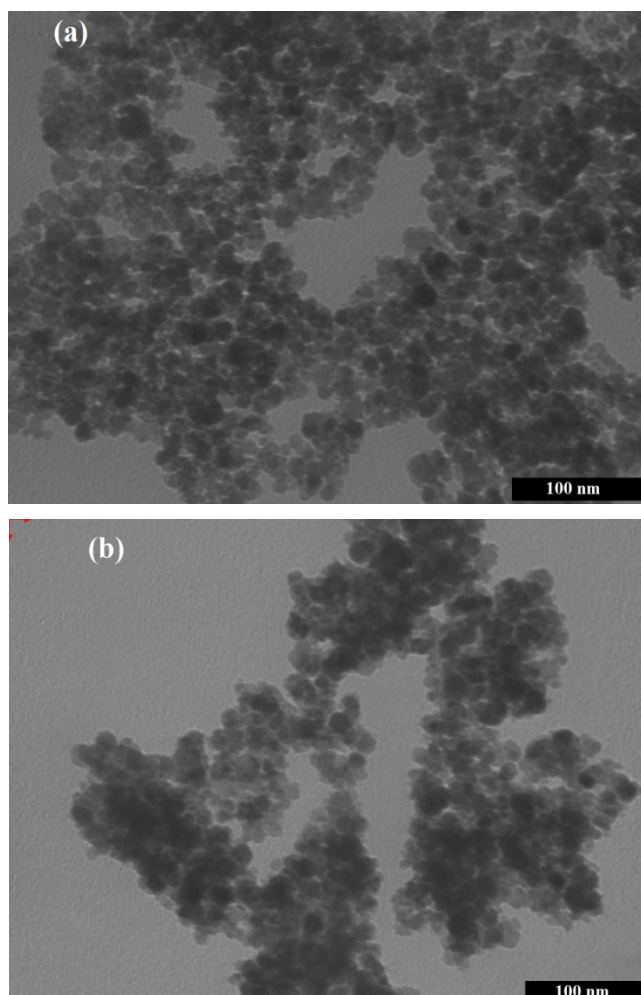


**Figure 3.** TEM of MNPs (a) and MNPs-APTES (b).

measurements.

### 3.3. XRD Studies

**Figure 4** shows the XRD patterns of MNPs and MNPs-APTES. The diffraction peaks at ( $2\theta = 30.29^\circ, 35.69^\circ, 43.30^\circ, 53.69^\circ, 57.38^\circ, 64.8^\circ$  and  $74.58^\circ$ ) which corresponds to (220), (311), (400), (422), (511), (400), and (533) can be easily indexed to a cubic spinel structure of magnetite according to the standard XRD pattern of MNPs (JPCDS card, file No. 77 - 1545) [20]. It was also an evident that the APTES coating of the MNPs did not lead to a phase change of MNPs. The average crystallite size of MNPs-APTES is estimated about 30 nm according to linewidth of the (311) plane refraction peak using Scherrer's formula,  $D = (0.94\lambda/B \cos\theta)$

Where D is the average crystalline diameter, 0.94 is the Scherrer constant,  $\lambda$  the X-ray wavelength ( $\lambda = 0.154$  nm), B is half width of XRD diffraction lines and  $\theta$  is the Bragg's angle in degree. Accordingly, the average crystallite size was in good agreement with the TEM analysis.

### 3.4. Magnetic Measurements

**Figure 5** shows the magnetization curve of MNPs-APTES at room temperature. The S-shape of MNPs-APTES exhibited zero coercivity and permanence indicating its superparamagnetism with a saturation magnetization ( $M_s$ ) value 41.5 emu/g, which can be ascribed to the existence of APTES on surface of MNPs. Therefore, This MNPs-APTES having magnetic response could be carry drugs to targeted locations under an external magnetic field. The determined magnetic separation time is about 15 s.

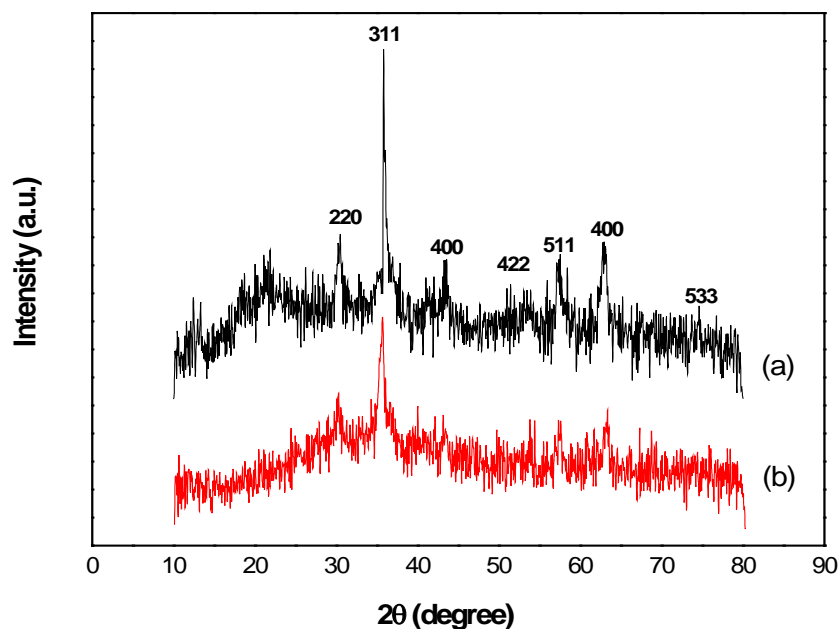


Figure 4. XRD of MNPs (a) and MNPs-APTES (b).

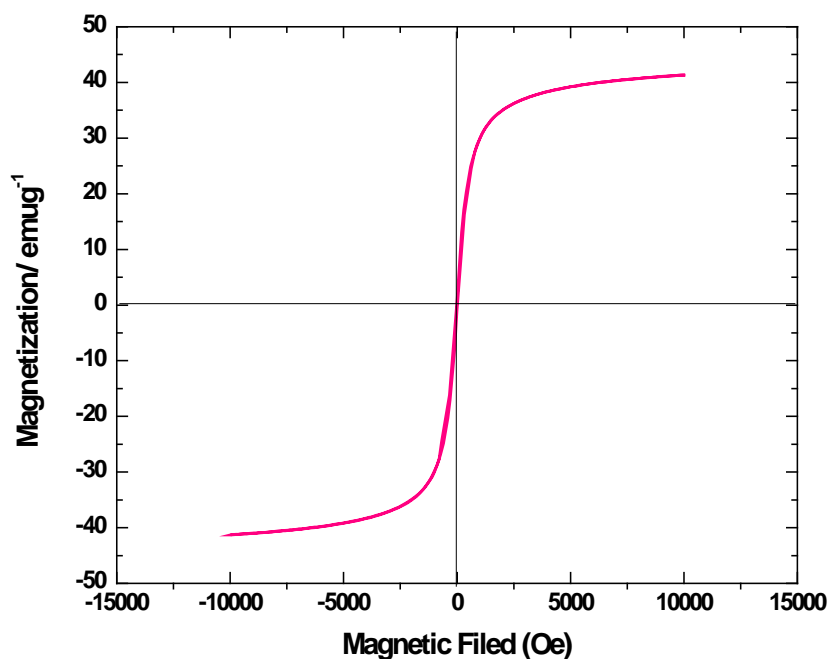
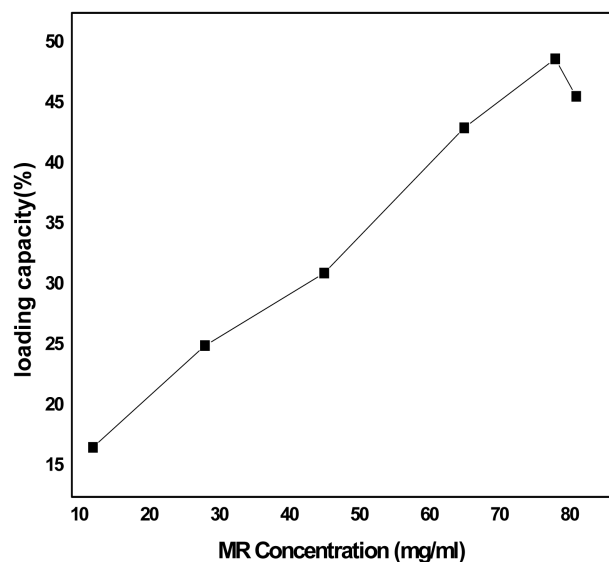


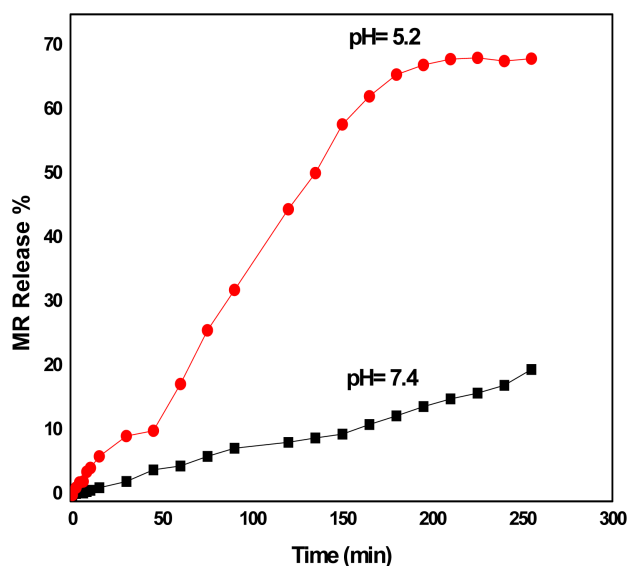
Figure 5. Magnetisation curve of MNPs-APTES at room temperature.

### 3.5. Drug Loading and Release Studies

The drug loading and release behavior of MNPs-APTES are shown in **Figure 6(a)** and **Figure 6(b)**. In **Figure 6(a)** loading profile, the percentage of loaded MR increased and reached the maximal value of 48.7% for 78 mg/mL MR. This due to the conjugated of hydroxyl group in MR to the active amino group in the surface of MNPs-APTES (**Figure 1**). The drug released profile of MR from MNPs-APTES was studied in PBS with a pH of (5.2 and 7.4) at  $37^\circ\text{C}$ , respectively. As seen in **Figure 6(b)**, approximately 68.2% MR was released from MNPs-APTES within 4 h at pH 5.2 whereas, 19.6% of drug was released at pH 7.4. Thus, the drug release at



(a)



(b)

**Figure 6.** Morin loading on MNPs-APTES (a) and morin release from MNPs-APTES (b).

pH 5.2 was much faster than that at pH 7.4. It may be due to the protonation of amine groups under this environment.

#### 4. Conclusion

The novelty of this study is the successful binding of MR to MNPs-APTES. Characterization of the drug delivery system was carried out by FTIR, TEM, XRD, DLS, and VSM techniques. Spherical iron oxide nanoparticles were synthesized by co-precipitation technique and coated with APTES solution. The TEM analysis revealed that the average particle size increased to 26.7 nm after APTES coating. Moreover, the mean particle size of MNPs-APTES obtained from DLS was larger than that obtained from TEM analysis. The drug loading and release behavior of MNPs-APTES showed that the maximal value of the drug loading capacity was approximately 48.7% and the *in vitro* release behavior of drug presented that 68.2% and 19.6% were released in acidic

and neutral buffered solutions at pH (5.2 and 7.4), respectively within 4 h. Thus, MNPs-APTES can be used as a potential carrier targeted morin anticancer drug delivery applications.

## Acknowledgements

The authors would like to thank the financial support of the National Natural Foundations of China (No.21175086 and No.21175087), School of International Education and Exchange and Shanxi University.

## References

- [1] Manju, S., Sharma, C.P. and Sreenivasan, K. (2011) Targeted Coadministration of Sparingly Soluble Paclitaxel and Curcumin into Cancer Cells by Surface Engineered Magnetic Nanoparticles. *Journal of Materials Chemistry*, **21**, 15708-15717. <http://dx.doi.org/10.1039/c1jm12528a>
- [2] Iida, H., Takayanagi, K., Nakanishi, T. and Osaka, T. (2007) Synthesis of Fe<sub>3</sub>O<sub>4</sub> Nanoparticles with Various Sizes and Magnetic Properties by Controlled Hydrolysis. *Journal of Colloid and Interface Science*, **314**, 274-280. <http://dx.doi.org/10.1016/j.jcis.2007.05.047>
- [3] Weissleder, R., Bogdanov, A., Neuwelt, E. and Papisov, M. (1995) Long Circulating Iron Oxides for MR Imaging. *Advanced Drug Delivery Reviews*, **16**, 321-334. [http://dx.doi.org/10.1016/0169-409X\(95\)00033-4](http://dx.doi.org/10.1016/0169-409X(95)00033-4)
- [4] Jain, T.K., Roy, I., De, T.K. and Maitra, A. (1998) Nanometer Silica Particles Encapsulating Active Compounds: A Novel Ceramic Drug Carrier. *Journal of the American Chemical Society*, **120**, 11092-11095. <http://dx.doi.org/10.1021/ja973849x>
- [5] Sang, Q., Luan, L., Feng, S., Yan, H. and Liu, K. (2012) Using a Bifunctional Polymer for the Functionalization of Fe<sub>3</sub>O<sub>4</sub> Nanoparticles. *Reactive and Functional Polymers*, **72**, 198-205. <http://dx.doi.org/10.1016/j.reactfunctpolym.2012.01.003>
- [6] Katz, E., Weizmann, H. and Willner, I. (2005) Magneto Switchable Reactions of DNA Monolayers on Electrodes: Gating the Processes by Hydrophobic Magnetic Nanoparticles. *Journal of the American Chemical Society*, **127**, 9191-9200. <http://dx.doi.org/10.1021/ja0517771>
- [7] Heng, G.F., Zhao, J., Tu, Y.H., He, P.G. and Fang, Y.Z. (2005) Sensitive DNA Electrochemical Biosensor Based on Magnetite with a Glassy Carbon Electrode Modified by Multi-walled Carbon Nanotubes in Polypyrrole. *Analytica-Chimistry Acta*, **533**, 11-16.
- [8] Zhu, A.P., Yuan, L.H. and Liao, T.Q. (2008) Suspension of Fe<sub>3</sub>O<sub>4</sub> Nanoparticles Stabilized by Chitosan and O-carboxymethylchitosan. *International Journal of Pharmaceutics*, **350**, 361-368. <http://dx.doi.org/10.1016/j.ijpharm.2007.09.004>
- [9] Deng, H., Li, X.L., Peng, Q., Wang, X., Chen, J.P. and Li, Y.D. (2005) Monodisperse Magnetic Single-Crystal Ferrite Microspheres. *Angewandte Chemie International Edition*, **44**, 2782-2785. <http://dx.doi.org/10.1002/anie.200462551>
- [10] Smith, E.A. and Chen, W. (2008) How to Prevent the Loss of Surface Functionality Derived from Amino Silan. *Langmuir*, **24**, 12405-12409. <http://dx.doi.org/10.1021/la802234x>
- [11] Rice-Evans, C., Miller, N.J. and Paganga, G. (1996) Structure-Antioxidant Activity Relationships of Flavonoids and Phenolic Acids. *Free Radical Biology & Medicine*, **20**, 933-956. [http://dx.doi.org/10.1016/0891-5849\(95\)02227-9](http://dx.doi.org/10.1016/0891-5849(95)02227-9)
- [12] Fang, S.H., Hou, Y.C., Chang, W.C., Hsiu, S.L., Chao, P.D. and Chiang, B.L. (2003) Morin Sulfates/Glucuronides Exert Anti-Inflammatory Activity on Activated Macrophages and Decreased the Incidence of Septic Shock. *Life Sciences*, **74**, 743-756. <http://dx.doi.org/10.1016/j.lfs.2003.07.017>
- [13] Hanasaki, Y., Ogawa, S. and Fukui, S. (1994) The Correlation between Active Oxygens Scavenging and Antioxidative Effects of Flavonoids. *Free Radical Biology & Medicine*, **16**, 845-850. [http://dx.doi.org/10.1016/0891-5849\(94\)90202-X](http://dx.doi.org/10.1016/0891-5849(94)90202-X)
- [14] Sivaramakrishnan, V. and Devaraj, S.N. (2010) Morin Fosters Apoptosis in Experimental Hepatocellular Carcinogenesis Model. *Chemico-Biological Interactions*, **183**, 284-292. <http://dx.doi.org/10.1016/j.cbi.2009.11.011>
- [15] Yu, Z., Fong, W.P. and Cheng, C.H.K. (2006) The Dual Actions of Morin (3,5,7,2',4'-Pentahydroxyflavone) as a Hypouricemic Agent: Uricosuric Effect and Xanthine Oxidase Inhibitory Activity. *Journal of Pharmacology and Experimental Therapeutics*, **316**, 169-175. <http://dx.doi.org/10.1124/jpet.105.092684>
- [16] Liu, X., Ma, Z., Xing, J. and Liu, H. (2004) Preparation and Characterization of Amino-Silane Modified Superparamagnetic Silica Nanospheres. *Journal of Magnetism and Magnetic Materials*, **270**, 1-6. <http://dx.doi.org/10.1016/j.jmmm.2003.07.006>
- [17] Cao, H., He, J., Deng, L. and Gao, X. (2009) Fabrication of Cyclodextrin Functionalized Superparamagnetic Fe<sub>3</sub>O<sub>4</sub>/Amino-Silane Core-Shell Nanoparticles via Layer-by-Layer Method. *Applied Surface Science*, **255**, 7974-7980.

<http://dx.doi.org/10.1016/j.apsusc.2009.04.199>

- [18] Ma, M., Zhang, Y., Yu, W., Shen, H.Y., Zhang, H.Q. and Gu, N. (2003) Preparation and Characterization of Magnetite Nanoparticles Coated by Amino Silane. *Colloids and Surface A*, **212**, 219-226. [http://dx.doi.org/10.1016/S0927-7757\(02\)00305-9](http://dx.doi.org/10.1016/S0927-7757(02)00305-9)
- [19] Yamaura, M., Camilo, R.L., Sampaio, L.C., Macedo, M.A., Nakamura, M. and Toma, H.E. (2004) Preparation and Characterization of (3-Aminopropyl) Triethoxysilane-Coated Magnetite Nanoparticles. *Journal of Magnetism and Magnetic Materials*, **279**, 210-217. <http://dx.doi.org/10.1016/j.jmmm.2004.01.094>
- [20] Das, M., Mishra, D., Maiti, T.K., Basak, A. and Pramanik, P. (2008) Bio-Functionalization of Magnetite Nanoparticles Using an Aminophosphonic Acid Coupling Agent: New, Ultradispersed, Iron-Oxide Folate Nanoconjugates for Cancer-Specific Targeting. *Nanotechnology*, **19**, Article ID: 415101. <http://dx.doi.org/10.1088/0957-4484/19/41/415101>